ISSN 2075-1087, Gyroscopy and Navigation, 2025, Vol. 16, No.2, pp. 168–176
Original Russian Text D.A. Koshaev and V.V. Bogomolov published in Giroskopiya i Navigatsiya, 2025, Vol. 33, No. 2, pp. 91–102

Long Baseline Underwater Positioning with Fusion of Saved and Current Measurements and Ambiguity Resolution. Part 2. Performance Evaluation

D. A. Koshaev[a,*] and V. V. Bogomolov[a, b]

[a]*Concern CSRI Elektropribor, JSC, St. Petersburg, Russia*
[b]*ITMO University, St. Petersburg, Russia*
**e-mail: dkoshaev@yandex.ru*

Received: December 17, 2024; reviewed: March 24, 2025; accepted: April 1, 2025

Abstract: The results of the testing of the algorithm for determining the position of an autonomous underwater vehicle (AUV) using measurements of ranges to acoustic beacons and data from a water-speed log and heading indicator, proposed in Part 1, are considered. The essential features of the algorithm are that it starts running without a priori AUV coordinates and without a set of simultaneous measurements required to obtain an unambiguous navigation solution, recursive processing of current measurements and the measurements saved before the solution started in the same filter, taking into account the AUV position ambiguity and its resolution. The runtime of the proposed algorithm is compared with other possible solutions. The results of the simulation and field data postprocessing have made it possible to evaluate the time needed to obtain the first unambiguous solution and the accuracy of unambiguous solutions obtained with the use of the developed algorithm for different number and locations of acoustic beacons and AUV trajectories. Two types of desynchronization of the beacons and AUV clocks are considered: random and unknown; accordingly, either range or range-difference measurements are used. The solutions with and without taking into account the measurements saved before the algorithm started are compared.

Keywords: autonomous underwater vehicle, long baseline method, range and range-difference measurements, dead reckoning, Kalman filter, ambiguity, a posteriori probability, simulation, field data postprocessing.

INTRODUCTION

In Part 1 of this article [1], the authors formulated the mathematical problem statement for determining AUV coordinates based on the long baseline (LBL) method. The problem involves conditions that are nonstandard for the application of this method: the number of available beacons and their arrangement relative to the AUV do not allow obtaining an unambiguous navigation solution based on simultaneous measurements. It is supposed that there are no a priori coordinates of the AUV that would allow choosing an unambiguous solution. The desynchronization between the beacons and the AUV clocks is assumed to be random (constant + white noise) with known characteristics or represents an unknown value. For unknown desynchronization, range-difference measurements are used in the processing. The first part of the article contains a detailed description of the algorithm for the problem solution, which combines nonlinear (including multiple model) and linear estimation methods to obtain a computationally simple solution that can be implemented in the AUV onboard hardware in real time.

This article, which is Part 2 of [1], is devoted to the study of the algorithm proposed and discussed in Part 1; it consists of three sections. In Section 1, we compare the runtime of our algorithm with other solutions that also, like the proposed algorithm, provide processing of both current measurements and measurements saved before the algorithm startup, hereinafter called saved measurements. Sections 2 and 3 present the results of the algorithm numerical testing obtained by simulation of a set of random samples of measurement errors and field data postprocessing. The solutions with and without account of saved measurements are compared. In so doing, basically, we consider scenarios with ambiguity in determining the AUV coordinates. The results are analyzed in terms of the time needed to obtain the first unambiguous solution and the accuracy of unambiguous solutions. In the simulation, we deal with the root-mean-square errors (RMSE) of coordinate estimates. The actual RMSE obtained

from the samples of the coordinate estimate errors are compared with the calculated RMSE obtained from the covariance matrices generated in the algorithm [2]. In addition to RMSE, we determine the proportion of unambiguous solutions from the total number of the simulated solutions.

1. EVALUATION OF THE ALGORITHM RUNTIME

In this section, the time required to implement the algorithm described in Part 1 of the article is compared with that needed for other algorithms that also recursively process the previously saved measurements before the solution started, at a single noninitial step of the algorithm (after the arrival of measurement vector Y_1, Y_2, etc.). Desynchronization δ of clocks was assumed to be random, that is, original range measurements were processed directly. Before the solution started, measurements were obtained from one beacon, and after start, from two beacons. Calculations of the ratio of posterior probabilities of hypotheses for an ambiguous solution were not taken into account in the comparison.

Two algorithms were considered as alternatives to the proposed one. The first algorithm includes two Kalman filters (KF), one of which processes current measurements in forward time, while the other one processes saved measurements in backward time. The data of the two filters are fused using the dummy measurements method [3, 4]. The second algorithm differs from the algorithm with two KFs in that saved measurements are processed by fixed-point smoothing (FPS) [5,6] instead of the KF. The fixed point is the time when the solution starts. We analyzed two variants for each of the alternative algorithms. In the first one, two KFs or FPS with the KF, denoted as ←KF+KF→, ←FPS+KF→, are used in turn; in the second variant, they work in parallel: ←KF||KF→, ←FPS||KF→. It should be borne in mind that parallel computing technology cannot always be implemented in the AUV onboard computer, since it requires special hardware and software. The algorithm proposed in the article provides for processing of current measurements in forward time and those saved before the solution started, in backward time using the same KF, which is why we designate it as ←KF→. The algorithms runtimes were evaluated with different numbers of ΔN of the saved measurements processed in one i-step of the solution. Clearly, the algorithms ←KF||KF→, ←FPS||KF→ are most effective at $\Delta N = 1$, when the amount of parallel calculations in them for forward and backward time are comparable. As ΔN increases, the differences in the performance between ←KF||KF→ and ←KF+KF→, ←FPS||KF→ and ←FPS+KF→ should obviously level off.

The diagram in Fig. 1 shows ratio of the runtime of the algorithms ←KF+KF→, ←KF||KF→, ←FPS+KF→, ←FPS||KF→ to the runtime of the algorithm ←KF→. We should keep in mind that this ratio varies depending on the hardware and software. The state vector dimensionality may also affect runtime. In this regard, the data provided cannot be extended to the onboard versions of the algorithms, but they give an approximate idea of the relative performance of all the algorithms mentioned.

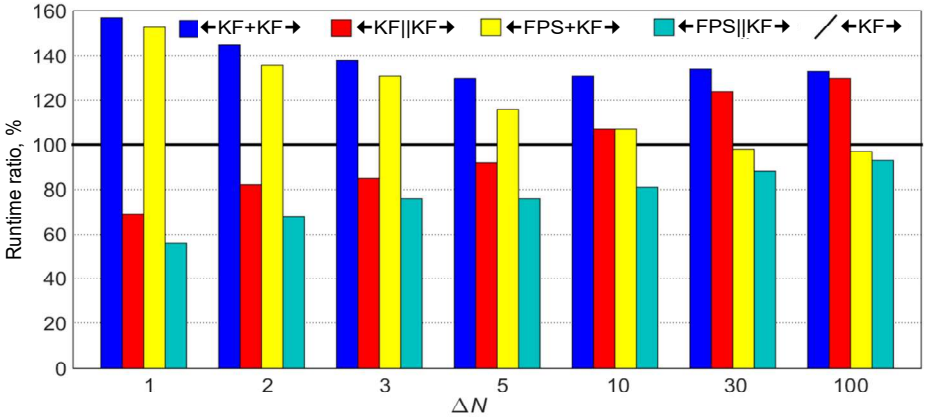

Fig. 1. Runtime ratios of the four algorithms and the algorithm ←KF→ at a single noninitial step of solution.

In general, we can say that the solutions under consideration do not have any fundamental differences in their performance. Algorithm ←KF→ has a certain advantage over the alternative ones that do not use parallel computing. Compared to ←KF+KF→, algorithm ←KF→ wins in performance by 30–60%

for all considered $\Delta N \le 100$. As distinct from ←FPS+KF→, the results of algorithm ←KF→ are 30–50% better only for $\Delta N \le 3$. Algorithm ←FPS||KF→ is the most efficient of the presented algorithms; it outperforms ←KF→ by 20–50% for $\Delta N \le 10$, but with a further increase in ΔN, its superiority vanishes.

At the same time, it was found that the time spent on the solution startup ($i = 0$) with $n_0 = 2$, $L = 12$ to obtain $\breve{\mathbf{x}}_0^{(l)}, \breve{\mathbf{y}}_0^{(l)}$ from $\tilde{\mathbf{x}}_0^{(l)}, \tilde{\mathbf{y}}_0$, $l = \overline{1,L}$ with 5 iterations (stage 2, section 2 in [1]) turns out to be less, but comparable with the runtime of the considered algorithms at a noninitial step with $\Delta N = 100$, if $\breve{\mathbf{x}}_0^{(l)}, \breve{\mathbf{y}}_0^{(l)}$ are calculated sequentially. In the case of parallel computing of $\breve{\mathbf{x}}_0^{(l)}, \breve{\mathbf{y}}_0^{(l)}$, this time is significantly reduced. The time needed to calculate the ratio of a posteriori probabilities of hypotheses $\delta p_i^{1/2}$ is much less than the total runtime of the algorithms for $\Delta N = 1$.

2. SIMULATION

The proposed algorithm was simulated in different navigation situations, each with random and unknown desynchronization δ of the beacon and AUV clocks. The AUV ground speed was set equal to 5 m/s. In each example, the simulation was based on 1500 samples of random errors in range measurements, data from the heading indicator and log, as well as errors in the current speed knowledge. Error parameters were as follows: range measurement noise with standard deviation (SD) of $\sigma_v = 10$ m, constant error in the sound speed knowledge with $\sigma_{\Delta c} = 3$ m/s, log measurement noise with $\sigma_{\Delta V} = 0.1$ m/s, slowly changing errors in determining the heading with $\sigma_{\Delta K} = 5°$, and in the knowledge of the current speed components with $\sigma_{\Delta U} = 0.25$ m/s; correlation intervals of these components $\tau_{\Delta U} = \tau_{\Delta K} = 3600$ s. In the case of random desynchronization, the SD of its constant component was $\sigma_b = 20$ m, and for the noise component, it was $\sigma_e = 2$ m. The measurement sampling interval was $\Delta t_i = 1$ s. Acoustic measurements were simulated only in the cases when the distance from the beacon to the AUV did not exceed 1 km. The algorithm had the following parameters: the assumed maximum signal reception range from beacons was $D_{\max} = 1.5$ km; the parameter determining the preliminary estimate grid step was $\delta\bar{\mathbf{x}} = 300$ m; the number of saved measurements processed at the first step of the solution after the algorithm startup was $\Delta N_0 = 0$ (i.e. they are not processed until the measurement vector Y_1 is obtained) and at noninitial steps (after Y_1, Y_2, etc. is obtained), $\Delta N = 10$; the threshold for the ratio of the a posteriori probabilities of the hypotheses about the AUV position was $\delta\bar{p} = 10^4$ for random desynchronization and $\delta\bar{p} = 10^5$ for unknown desynchronization. Recall that D_{max} and $\delta\bar{\mathbf{x}}$ are used to determine the boundaries of the preliminary estimates when the algorithm is launched (see the explanations for expressions (8) in [1]). If the ratio of the larger a posteriori probability to the smaller one exceeds the threshold $\delta\bar{p}$, the more probable hypothesis is accepted as a true one and the solution is considered unambiguous (see the rule for choosing the true hypothesis at the beginning of Section 4 in [1]).

The simulation results are presented in Figs. 2–4 in the same format. The graphs at the top left show the beacons, true trajectory, a sample of a trajectory for the false hypothesis about the AUV position, which is considered before the ambiguity resolution without account of the saved measurements, and lines of position-circles and hyperbolas for the range and range-difference measurements at the moment when the solution starts. The term ‘range-difference measurements’ is used in reference to differences between the range measurements from beacons 2, 3 and beacon 1. The two upper graphs on the right show the actual (from the samples of the estimation errors) and calculated (from the KF covariance matrices) RMSE [2] of coordinate estimates obtained for a set of solutions generated by the algorithm under consideration with and without account of the measurements saved before the algorithm is launched. This RMSE is given only for unambiguous solutions, i.e. for those in which, by that time, the true hypothesis about the possible AUV position was chosen. For this reason, the RMSE graphs do not begin from the start of the algorithm, when the number of unambiguous solutions is small. The third graph on the top right shows the proportion of unambiguous solutions of all 1500 simulated ones. The horizontal axis on the graphs shows the time passed from the moment t_0, when the solution started. At the bottom of the figures are the graph of the AUV heading and the diagram of the beacons used. In the simulation, we studied Cases A, D2, and B2 introduced in [1], where it was impossible to determine the AUV unambiguous position at the beginning of the solution.

First, let us make some general comments on the simulation results. It is evident from the RMSE graphs that the calculated RMSE adequately conveys the real level of error. The discrepancies between the calculated and actual RMSE are noticeable, but insignificant. The unambiguous solutions obtained during the simulation were correct, i.e. of the two hypotheses about the AUV position, the true one was unmistakably chosen. Judging by the graphs of the percentage of unambiguous solutions in Figs. 2 and 3, processing of the saved measurements provides for faster ambiguity resolution. If we compare the RMSE of coordinates among unambiguous solutions, here, too, the algorithm taking into account the saved measurements has an advantage, which is especially obvious from the RMSE of x in Fig. 3 at the top. But this advantage decreases over time.

Further, we discuss individual examples of the solutions.

1. The results presented in Fig. 2, at the top, show that the AUV turns help resolve the ambiguity of solutions with random desynchronization δ and two beacons. In particular, the turn performed before the algorithm was launched made it possible to sharply increase the number of unambiguous solutions provided that the saved measurements were taken into account in the algorithm. The ambiguity of the AUV position is resolved owing to the fact that for the true hypothesis, the new incoming acoustic measurements agree with the AUV coordinate prediction estimates based on data from the log and heading indicator, whereas for the false hypothesis, the measurements and predicted coordinates increasingly contradict each other over time. In the example at the top of Fig. 2, the straight section of the trajectory on which the solution begins has a small inclination (10 deg) to the straight line passing through beacons 1 and 2, which complicates the ambiguity resolution. As this trajectory inclination increases, as in the example at the bottom of Fig. 2, where it is 60 deg, the ambiguity is resolved faster. When the saved measurements are taken into account in this example, this happens almost immediately. If the AUV moves in a straight line and parallel to the line passing through two beacons, the resolution of the ambiguity is impossible without a priori data on its coordinates.

2. With unknown desynchronization δ and three beacons, ambiguity resolution is possible for AUV rectilinear motion as well, even if it moves along a straight line connecting beacons 1 and 2, and beacon 3 is located with a small offset from this line (see Fig. 3 at the top). If the angle between the AUV trajectory and the straight line passing through beacons 1 and 2 increases to 60 deg (Fig. 3 at the bottom), the ambiguity is resolved almost as quickly as in a similar case with two beacons and random δ (Fig. 2 at the bottom). Note that in the example at the bottom of Fig. 3, the RMSEs of the coordinates with and without taking into account the saved measurements practically coincide, since the section before the start of the solution, where measurements can be saved, is rather short. And yet, unambiguous solutions are obtained faster with the use of the saved measurements.

3. Figure 4 shows the results for random desynchronization and three beacons located almost on the same line, which adversely affects the accuracy of the navigation solution and leads to ambiguity, since the lines of position in the form of three circles are close to intersection in two places. In this example, it was assumed that there were no measurements saved before the beginning of the solution, for example, because the whole navigation problem was started or restarted. In this example, when the solution started, the major semiaxis a of the calculated coordinate error ellipse exceeded the threshold of $\bar{a}$ = 500 m, and the solution was performed taking into account the ambiguity (see Case B in [1]). During the subsequent processing of the measurements, the ambiguity was resolved relatively quickly.

At the same time, it was found that in terms of coordinate RMSEs of unambiguous solutions, the proposed algorithm does not practically differ from the one in which all saved measurements are processed using the FPS procedure before processing of the current measurements [5, 6]. No significant differences in the results were found between the proposed algorithm and the one that uses two KFs for separate processing of current and saved measurements, and their fusion is performed using the method of dummy measurements [3, 4].

In closing this section, we note that the RMSE values shown in the graphs were obtained under the navigation conditions that are nonstandard for the application of the LBL method, so that these values cannot be compared with the error limit values of 10 m and less, which are considered typical for normal conditions.

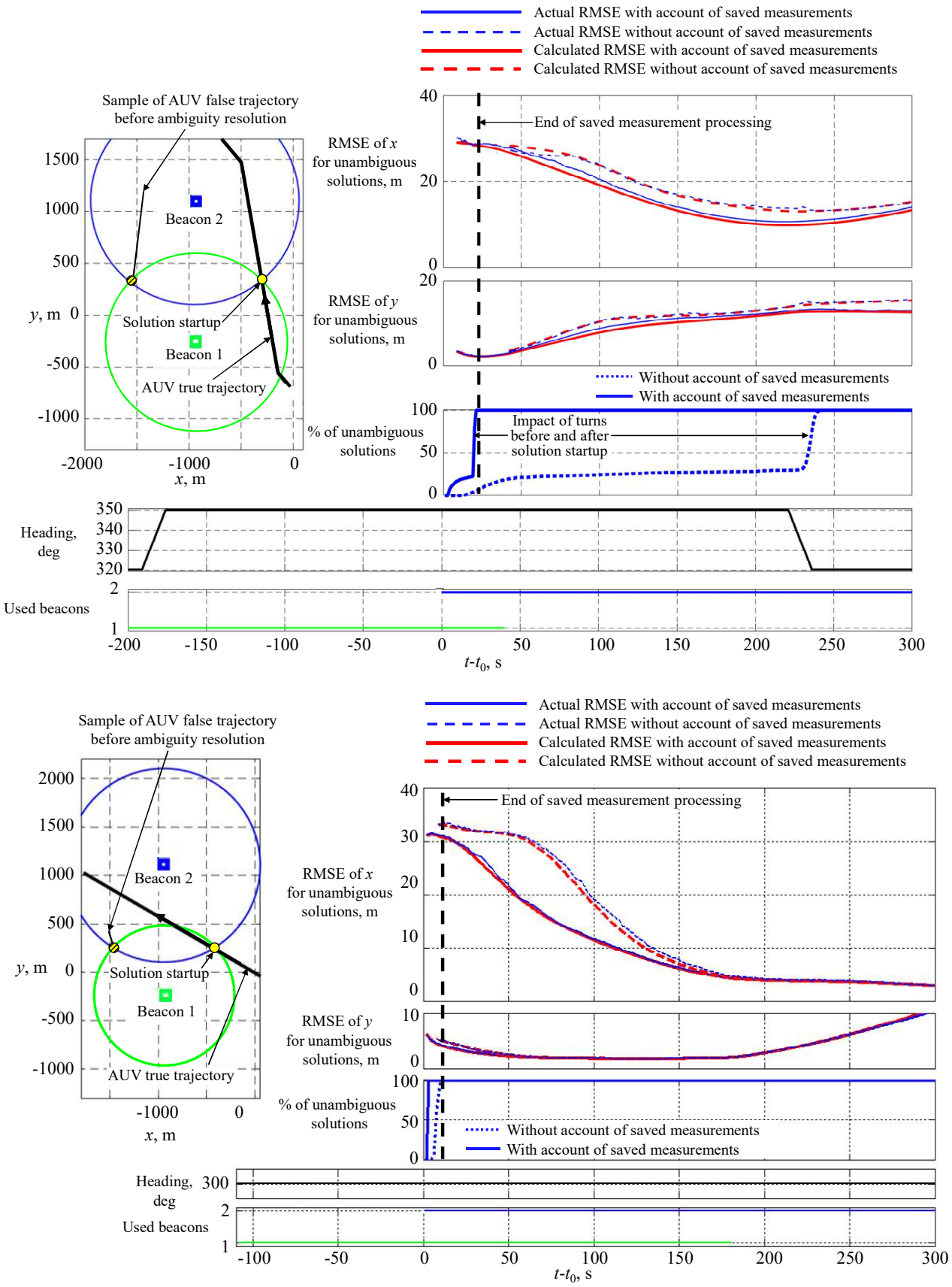

Fig. 2. Simulation conditions and results for random desynchronization of the beacon and AUV clocks in Case A [1] for different AUV trajectories.

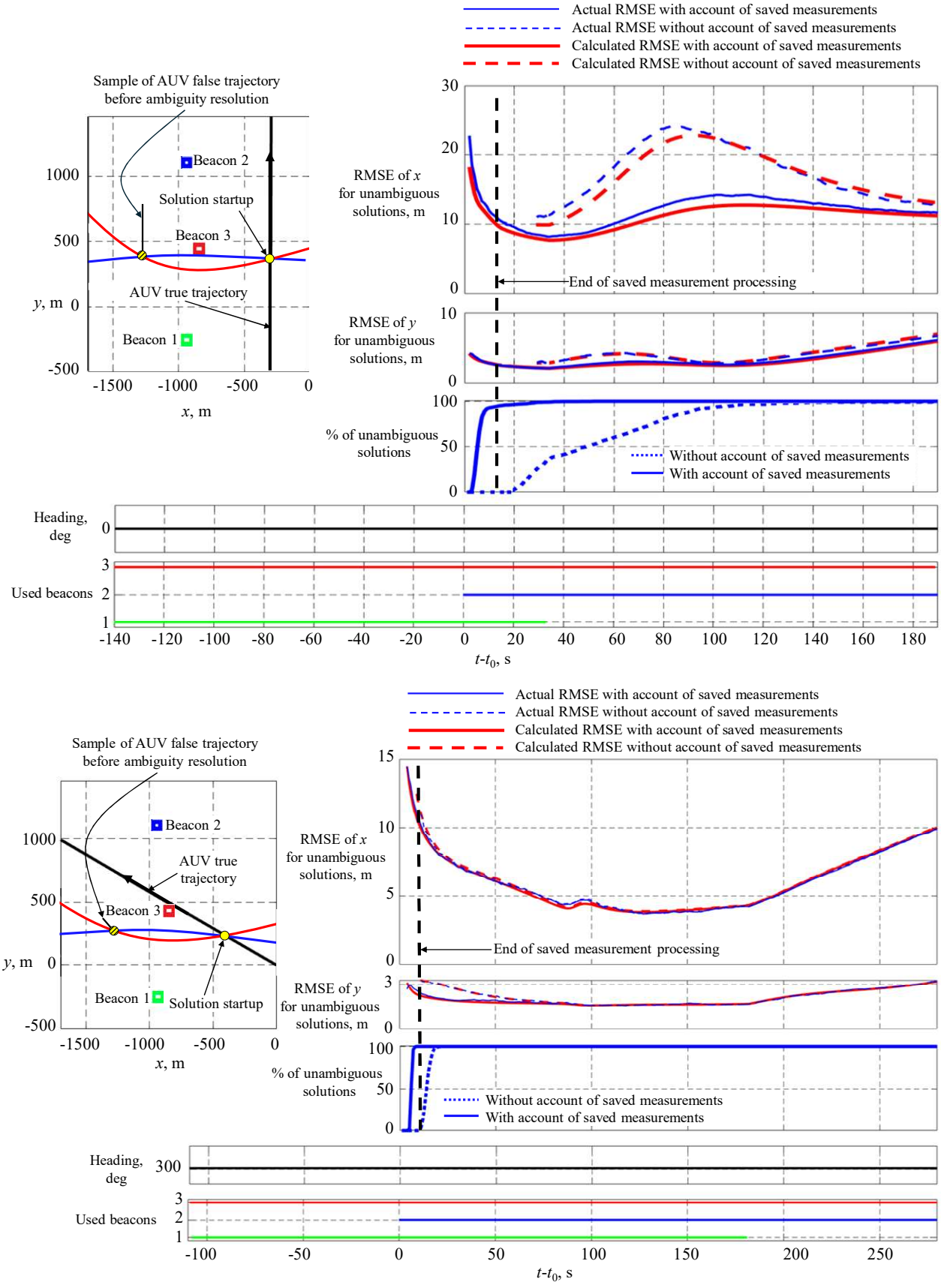

Fig. 3. Simulation conditions and results for unknown desynchronization of the beacons and AUV clocks in Case D2 [1] for different AUV trajectories.

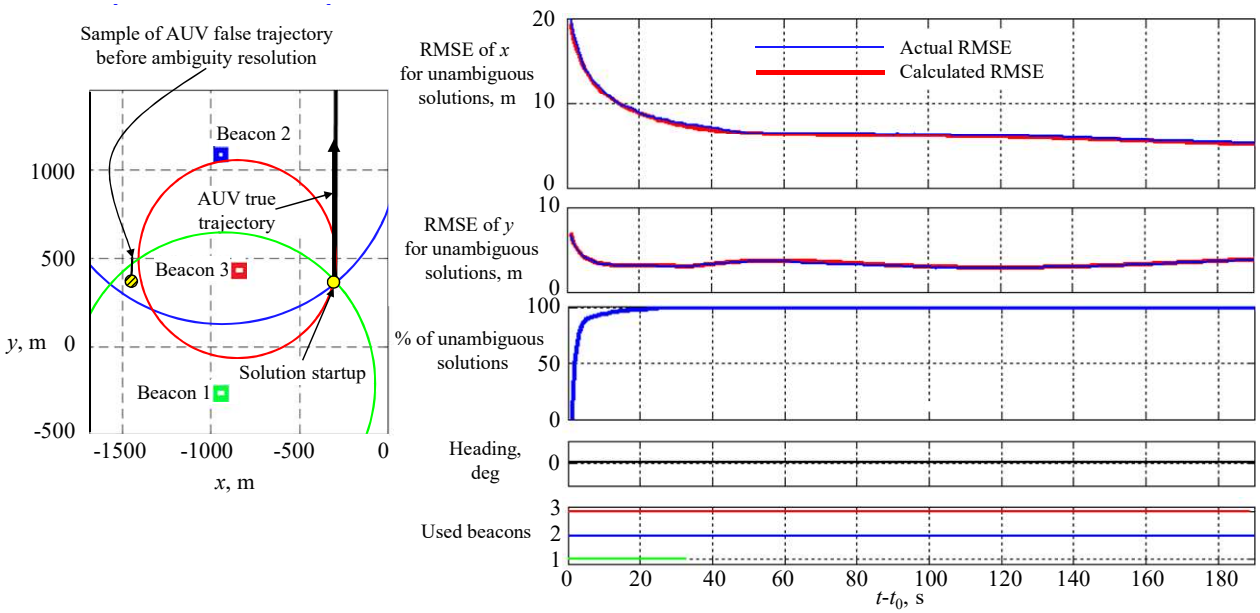

Fig. 4. Simulation conditions and results for random desynchronization of the beacons and AUV clocks in Case B2 [1].

3. FIELD DATA POSTPROCESSING

Figures 5 and 6 show the conditions and results of the experiments with the use of the field data processed in the office, with random and unknown desynchronization δ of the beacons and the AUV clocks. The field data were obtained from a boat equipped with a receiver of signals from Global Navigation Satellite Systems (GNSS). A towed underwater vehicle with an acoustic system was taken to imitate an AUV. In the experiment with random desynchronization, we used 2 beacons (Case A [1]) and 3 beacons were used in the case of unknown desynchronization (Case D1 [1]).

In the latter case, after the solution started, we had measurements only from one beacon. They were not used since it was impossible to form a range-difference measurement, and before the start, there were only 6 simultaneous measurements from two beacons (see the graph at the bottom of Fig. 6). Thus, here, after the solution started, rare saved measurements were processed for 28 s, whereas the solution without account of the saved measurements was reduced to the dead reckoning (prediction), which was based on the initial solution obtained with the use of measurements from three beacons.

As in the simulation, we considered solutions with and without account of saved measurements. The speed of the towed vehicle was about 4 m/s. Its reference coordinates were calculated based on the coordinates provided by the GNSS receiver and the known length of the cable. Since the dead reckoning used the geographic components of absolute velocity from the GNSS receiver, the errors of the heading and current speed components are absent and are not estimated in the problem. The rest of the calculations with field data were carried out with the same algorithm parameters as in the simulation. In the problem with random desynchronization, the measurements were complemented with the constant offset of $b = 30$ m (with $\sigma_b = 20$ m assumed in the algorithm).

The graphs in Figs. 5 and 6 are similar to those considered earlier for the simulation. The main difference is that the actual and calculated RMSE obtained from a set of solutions are replaced here for the sample of the estimation error and the tripled RMSE value obtained from the corresponding diagonal element of the KF covariance matrix. In the graphs for the heading and the number of the beacons used, the time scale before the solution startup is compressed as compared to the time scale after the solution started.

From the graphs of the coordinate estimation errors with random desynchronization (Fig. 5) it is evident that with account of the saved measurements, the ambiguity is resolved 2 s after the solution started, and without them, in 11 s. The angle between the direction of the AUV trajectory and the straight line passing through the two beacons in the experiment with random desynchronization is large enough to quickly obtain an unambiguous solution

despite the sparse diagram of the measurement arrivals. In the case of unknown desynchronization (Fig. 6), there is no ambiguity owing to the appropriate arrangement of the beacons and the AUV at the moment the measurements from three beacons arrive simultaneously.

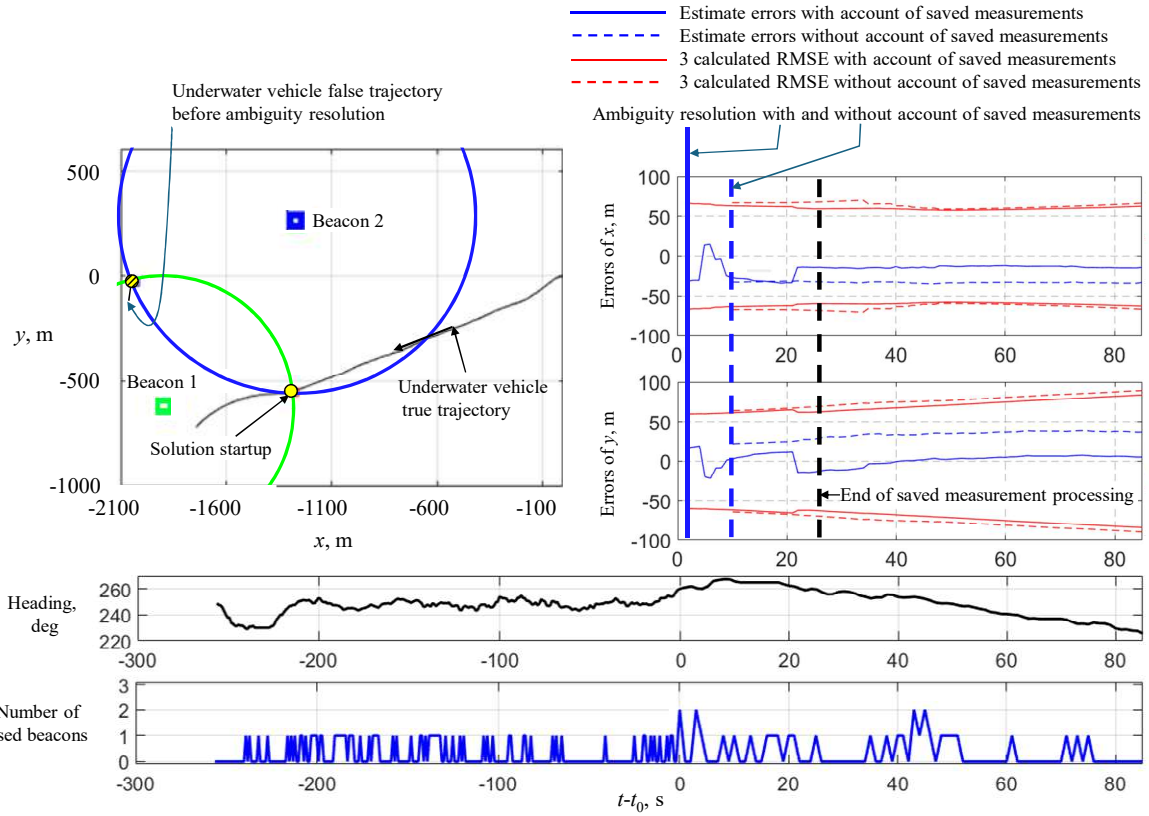

Fig. 5. Simulation conditions and results of the field data postprocessing for random desynchronization of the beacons and AUV clocks in Case A [1].

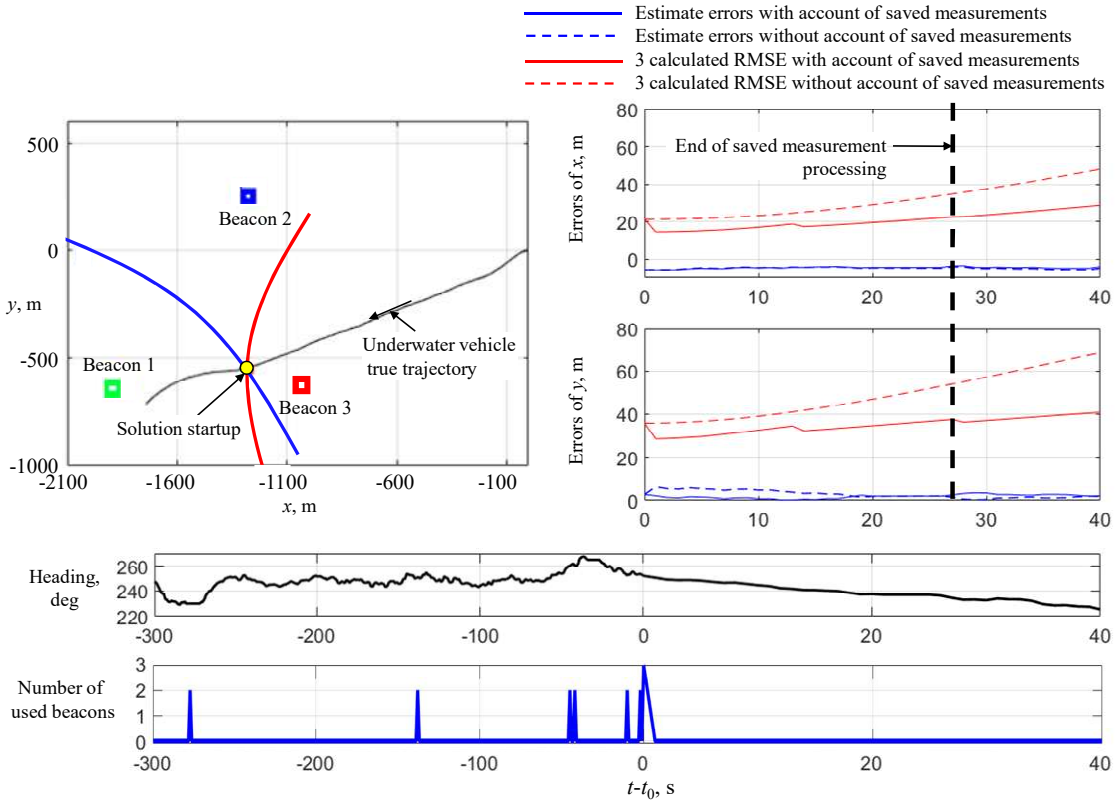

Fig. 6. Simulation conditions and results of the field data postprocessing for unknown desynchronization of the beacons and AUV clocks in Case D1 [1].

The errors in unambiguous solutions in the experiment with random desynchronization are considerably smaller when the saved measurements are taken into account, but in the case of unknown desynchronization, they do not significantly depend on this factor. The tripled calculated RMSEs exceed the actual level of error with a margin. Among other things, the results of field data postprocessing demonstrate the operability of the proposed algorithm in the case of a highly fragmented diagram of acoustic measurement arrivals.

CONCLUSIONS

The study described in Part 2 has confirmed the advantage of the developed algorithm, in the sense of runtime, over the other algorithms that process current and saved measurements (using two KFs or the FPS and KF) without parallel computing technology. It is noted that the initial ambiguous solution is computationally most difficult to obtain. The algorithm has been tested by the simulation of a set of random samples of measurement errors and field data postprocessing. It has been found that taking into account the measurements saved before the algorithm launch is primarily useful for reducing the time needed to obtain an unambiguous solution. It has been shown that in the situation with two beacons in use and random desynchronization of the beacons and AUV clocks, the time for obtaining unambiguous solutions is reduced when the AUV makes turns and when the angle between its trajectory and the straight line passing through the beacons increases. In the situation with three beacons and unknown desynchronization (processing of range-difference measurements), the ambiguity is resolved even when the beacons are located approximately on the same straight line and the AUV moves along it. It has been confirmed that the estimated RMSE adequately represents the actual level of error both in the simulation and in field data postprocessing.

FUNDING

This study was supported by the Russian Science Foundation (project no. 23-19-00626), https://rscf.ru/project/23-19-00626/.

CONFLICT OF INTEREST

The authors of this work declare that they have no conflicts of interest.

REFERENCES

1. Koshaev, D.A. and Bogomolov, V.V., Long baseline underwater positioning with fusion of saved and current measurements and ambiguity resolution. Part I. Mathematical formulation, *Gyroscopy Navig*., 2025, vol. 16, no.1, pp. 79–93. https://doi.org/10.1134/S2075108725700129
2. Stepanov, O.A. and Isaev, A.M., A procedure of comparative analysis of recursive nonlinear filtering algorithms in navigation data processing based on predictive simulation. *Gyroscopy Navig.*, 2023, vol. 14, no. 3, pp. 213–224. https://doi.org/10.1134/S2075108723030094
3. Koshaev, D.A., Method of dummy measurements for multiple model estimation of processes in a linear stochastic system, *Automation and Remote Control*, 2016, no. 6, pp. 1009–1030.
4. Bogomolov, V.V., AUV positioning with simultaneous processing of saved and current ranges to less than three acoustic beacons, *Podvodnye issledovaniya i robototekhnika*, 2024, no. 2, pp. 58–67. https://doi.org/10.37102/1992-4429_2024_48_02_07
5. Meditch, J., *Stochastic Optimal Linear Estimation and Control*, McGraw-Hill Inc., 1969.
6. Bogomolov, V.V. and Koshaev, D.A., AUV positioning algorithm by ranges to beacons insufficient for the simultaneous navigation solution, *Materialy 33 konferentsii pamyati vydayushchegosya konstruktora giroskopicheskikh priborov N.N. Ostryakova* (Proceedings of the 33rd Conference in Memory of N.N. Ostryakov), St. Petersburg: Elektropribor, 2022, pp. 66–69.